Moroccan Journal of Chemistry
ISSN: 2351-812X
http://revues.imist.ma/?journal=morjchem&page=login
Aman & al. / Mor. J. Chem. 6 N°3 (2018) 466-479

Thermodynamic parameter for steam reforming reaction of biodiesel by-product using nano-sized perovskite catalysts

D. Aman[(a)]*, D. R. Abd El-Hafiz[(a)], M. A. Ebiad[(a)]

[(a)] Egyptian petroleum Research Institute, PO box 11727, Cairo, Egypt,

** Corresponding author:*
dr.d_mohammad@yahoo.com
Received 27 Sept 2016,
Revised 12Jan 2018,
Accepted 18 Jan 2018

Abstract

The catalytic steam reforming of biodiesel by-product (glycerol) GSR for hydrogen production was carried out using perovskite nano-catalysts ($LaNiO_3$ and $LaCoO_3$). The two catalysts were prepared by the reverse microemulsion method and characterized by XRD, by TG/DTA, BET and HRTEM. Equilibrium product compositions of GSR reaction were determined at different reaction temperature (400-700°C) with glycerol: water molar ratio 1: 10 in a fixed-bed flow system under atmospheric pressure. The equilibrium constant and thermodynamics parameters (ΔG, ΔH and ΔS) were calculated. The results revealed that, the conversion of the glycerol gradually increases with reaction temperature until reached 100% at temperature 700°C. $LaNiO_3$ show higher gas product than $LaCoO_3$ at the same reaction temperature. Moreover, H_2 yield increased from 0.11 to 3.15 for $LaNiO_3$ and 0.01 to 1.33 for $LaCoO_3$. On the other hand, $LaCoO_3$ provided more deactivation resistant along to 16h than $LaNiO_3$. XRD analysis of spent catalysts revealed the presence of $La_2O_2CO_3$ phase. On using $LaNiO_3$, the produced product at 700°C was found to have a moderate calorific value (284.706 Btu/ft^3) as compared to high calorific value on using $LaCoO_3$ (434.785 Btu/ft^3) at 600°C due to the low yield of CO_2 (15 mol %).

Keywords: thermodynamic parameters, steam reforming, Glycerol, hydrogen, perovskite.

1.Introduction

The development of the technology utilizing biomass energy resources, attracts much attention due to the decrease of the fossil fuel "in the near future" will cause serious energy problems. Therefore, biodiesel gradually accepted as a replacement for petroleum-diesel [1]. An increase of biodiesel production led to a great increment of crude glycerol by-product, which represent about 10 wt% of the product produced during the catalytic transesterification process [2-3]. Glycerol steam reforming reaction is one of the most important methods that carried out by different authors [4-7] to convert glycerol by-product into renewable hydrogen. Hydrogen is widely used in the chemical and petroleum industries as well as a promising clean energy for electrical power generation and fuel cell devices [8]. Moreover, due to the complex glycerol Steam reforming reactions, a better system is requested for high-purity hydrogen production [9-14]. The purity of the hydrogen depends on reaction condition, such as temperature, pressure and steam to carbon ratio. Hence, to deep understanding the effects of reaction variables on hydrogen yield, complete thermodynamic analysis is required [15-17]. On the other hand, the selection of catalyst is an important factor that affects GSR reaction. Due to the high cost of noble metals and their less availability, promote the development of Co and Ni-based catalytic systems that inhibit coke formation [18]. A Perovskite type oxide (ABO_3) with a well-defined structure was an alternative to use metal-based precursors, in the order of nanometers, lessening the coke formation and increasing the activity of the catalysts [19]. Perovskite-type oxides (ABO_3) have redox properties, because a wide range of elements can be incorporated into the structure by partial substitution of A and/or B cations, giving rise to a combination of elements with different oxidation states [20]. Until now, the application of using $LaCoO_3$ peroviskite nano-catalysts to produce H_2 in the steam reforming of glycerol has not taken into consideration in the industrial processes. Therefore, in the present work, the variability of product distribution during catalytic steam reforming of glycerol to produce H_2 were investigated using $LaNiO_3$ and $LaCoO_3$ peroviskite nano-catalysts. The equilibrium concentrations (K) and thermodynamic parameter (ΔG, ΔH and ΔS) were calculated for the processes GSR at different reaction temperature 400–700^{o}C, glycerol: water ratio 1:10 and at atmospheric pressure. The stability of the prepared catalysts and the calorific value of the produced product also estimated.

2. Materials and methods

2.1. Catalyst preparation

Single-reverse microemulsion technique was used to prepare the two nano sized perovskite ($LaNiO_3$ and $LaCoO_3$) catalysts using cetyltrimethylammonium bromide CTAB as surfactant (S), 1-butanol as co-surfactant (CS), and cyclohexane as oil phase (O) according to the previous study [21]. To find the best microemulsions compositions for preparation of two proveskite catalysts, the triangle phase diagram studied as shown in Fig. (1). Firstly, aqueous solution of $LaCl_3.7H_2O$ and $Co(NO_3)_2.6H_2O$ or $Ni(NO_3)_2.6H_2O$ containing a total metal concentration of 1M (soln. W) was prepared. Solution W was added drop wise to different four solution, each of them contain CS:S = 1.5 mass ratio and different (S+CS):O mass ratios (=0.2 (A_1), 0.4 (A_2), 0.6 (A_3), and 0.8 (A_4)). The variation in conductivity due to addition of solution W into S+CS+O is an indicator for the emulsion phases, so, the conductivity was studied using a bench top Hanna conductivity meter kept at 25 ◦C with circulating water from a controlled temperature stabilizer. In the triangle diagram, (S+CS):(O) ratios located on the base of the triangle and the addition took place upwards along the dashed lines A_1–A_4. Only one point (S) have chosen, that corresponding to microemulsion A_4 to prepare the perovskite samples. Then, an aqueous NH_4OH solution (4M) added as a precipitating agent to the vigorously stirred microemulsion A_4 to obtain the corresponding perovskite. Finally, the produced mixture filtered, washed alternatively three times with a mixture of deionized water and alcohol, and dried at 100°C overnight. The dried powder grounded

in an agate mortar and calcined at 750 °C for $LaNiO_3$ and 800°C for $LaCoO_3$ for 4h under atmospheric conditions as verified from thermogravimetric analysis.

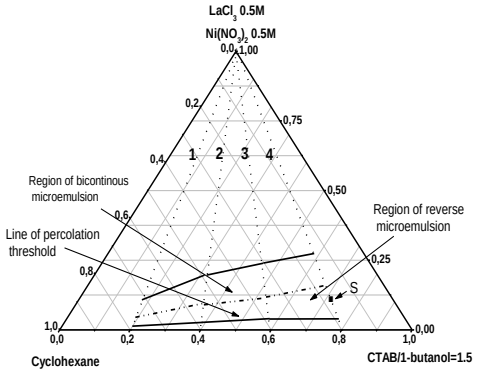

Figure. 1: Phase diagram of the reverse microemulsion system

2.2. Catalysts characterization

Thermal gravimetric analysis (TGA) carried out to using SETARAM Labsys TG-DSC16 model. X-ray powder diffraction Analysis (XRD) carried out using Shimadzu XD-1 diffractometer in 2θ range between 20 and 80°. The morphology of the samples was characterized by high-resolution transmission electron microscopy (HR-TEM) spectroscopy, the TEM pictures were obtained by a JEOL 2100F. N_2 adsorption-desorption isotherms and pore size distribution were derived from the low temperature nitrogen (-196°C) by Quantachrome NOVA2000 gas sorption analyzer, before adsorption measurements the samples were evacuated at 350°C for 24h.

2.3. Catalytic activity

The catalytic steam reforming of glycerol was carried out in a continuous flow system consists of a fixed bed tubular reactor working at atmospheric pressure. The reaction was examined for the two proveskite catalysts (0.2 g of the catalyst diluted with 0.2 g of the same sized quartz particles) at different reaction temperatures (400-700°C). Water/glycerol mixture (36% glycerol) fed into a preheater reactor (model SS316) at 150°C by a dosing pump with a flow rate of 0.1 ml/min using Nitrogen as carrier gas (40cm^3/min). The product stream was analyzed by the use of two gas Chromatographs (GC) (Agilent 6890 plus HP, Varian Natural Gas Analyzer type C model CP-3800) equipped with TCD and/or FID with three columns. A molecular sieve 5 Å capillary column used for the determination of H_2, oxygen, nitrogen, methane and carbon monoxide. While methane, carbon dioxide, ethane was analyzed by Hayesep P column. The third capillary column (DB-1) used for separation of methane, ethane, ethylene, acetaldehyde, ethanol, acetone.

- *Total conversion of glycerol (conversion to gas and liquid), selectivity, and yield of hydrogen, were evaluated according to the following equations:*

$$x(\%) = \frac{n_{C_3H_8O_3}in - n_{C_3H_8O_3}out}{n_{C_3H_8O_3}in} \times 100$$

$$x_{gasphase}(\%) = \frac{n_{CO_2}+n_{CO}+n_{CH_4}+n_{C_2H_4}}{3n_{C_3H_8O_3}in} \times 100$$

$$x_{liquidphase}(\%) = \frac{\sum_{i=1}(n_i x_i)}{3n_{C_3H_8O_3}in} \times 100$$

$$S_i(\%) = \frac{n_{i,out}}{n_{H_2,out} + n_{CO,out} + n_{CH_4,out} + n_{CO_2,out}} \times 100$$

$$H_2(yield) = \frac{H_2 \text{moles produced}}{\text{moles of glycerol fed}}$$

Where n_i corresponding to moles of species i and xi is the number of carbon atoms in the species i.

- *The calorific value of the obtained products at different reaction temperature calculated according to the ASTM 3588.*
- *The equilibrium constant (Kc) of all reactions were calculated using the equation:*

KC = [molar conc. of product]/ [molar conc. of reactant]

- *Thermodynamic parameters such as entropy and enthalpy were predicted by plotting the calculated values of lnKc vs. 1/T as follow:*

$$\ln K_C = \frac{\Delta S^0}{R} - \frac{\Delta H^0}{R}\frac{1}{T}$$

where ΔS^0 is the standard entropy (kJ mol^{-1} K^{-1}), ΔH^0 is the standard enthalpy (kJ mol^{-1}), R is the universal gas constant (J mol^{-1} K^{-1}) and T is the reaction temperature (K).

- *The standard state Gibbs free energy (ΔG^0) can be calculated as:*

$$\Delta G^0 = \Delta H^0 - T\Delta S^0$$

3. Results and Discussion

3.1. Catalyst characterization

X-ray diffraction patterns confirm the formation of $LaNiO_3$ and $LaCoO_3$ perovskite structure (Fig. 2). The high peak intensity was attributed to rhombohedral structures of $LaNiO_3$ and $LaCoO_3$ (JCPDS 33-0711) and (JCPDS file No. 48-0123), respectively [22, 23]. The disappearance of $La(OH)_3$ intermediate phase, confirmed that, the precursors are completely transformed into perovskite phase.

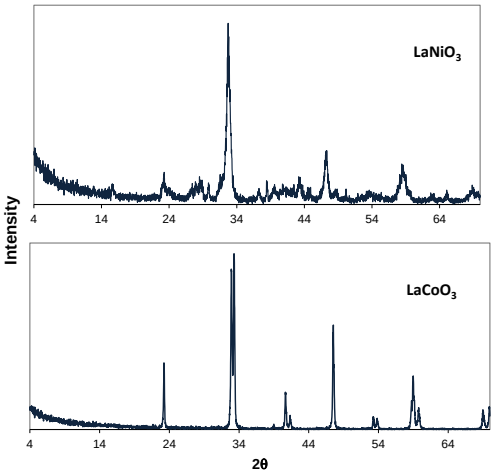

Figure. 2: XRD pattern for fresh $LaNiO_3$ & $LaCoO_3$ samples

The adsorption-desorption isotherm (Fig. 3), for both $LaNiO_3$ and $LaCoO_3$ are type II, according to the IUPAC classification, with H3 hysteresis loop, which indicate slit shaped pores [24, 25]. The small BET surface area of the two samples (Table 1), especially for $LaCoO_3$ (8.4 m^2/g), can be attributed to the high calcination temperature (800°C), moreover, this is an inherent characteristic of the perovskite-type oxides.

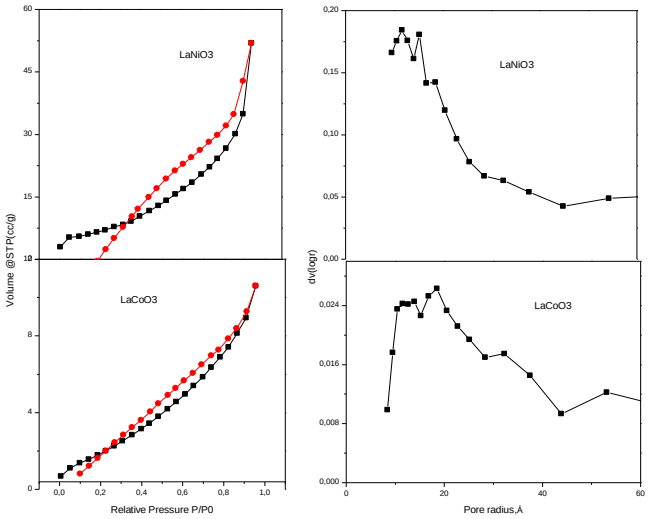

Figure. 3: Adsorption-desorption isotherms and pore size distribution for fresh $LaNiO_3$ and $LaCoO_3$

Table.1: BET surface area of the prepared catalysts

Perovskite	S_{BET} (m^2/g)	V_p (cm^3/g)	r_p (nm)
$LaNiO_3$	25.7	0.08	0.94
$LaCoO_3$	8.4	0.95	1.04

TEM images for both samples (Fig. 4), show a uniform particle size distribution with square particle shape. The grain sizes of the $LaNiO_3$ sample are 11–21 nm and that of the $LaCoO_3$ sample are 35–39 nm.

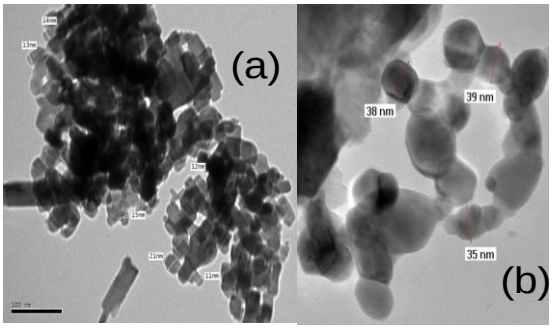

Figure . 4: TEM image for Fresh (a) $LaNiO_3$ and (b) $LaCoO_3$

3.2. Glycerol steam reforming

During glycerol steam reforming reaction (GSR), high selectivity to hydrogen can achieve by minimizing methane production and coke formation. Based on the thermodynamic analyses, applying the condition of high temperatures, low pressures and high water to glycerol molar ratios can confirm this idea [26, 27]. Thus, in this work, the catalytic GSR reaction was conducted under atmospheric pressure, at different reaction temperatures ranged from 400 to 700°C with glycerol: water molar ratio 1:10. The reaction then conducted for 16 h in order to assess the stability of the prepared catalysts toward GSR reaction. From data in Figure (5), it is clear that, after one hour and at a low reaction temperature the glycerol conversion over $LaNiO_3$ (78% at 400°C) is twice that over $LaCoO_3$ (40%) due to high surface area and small particle size of $LaNiO_3$. Then, the conversion increase with the increase of reaction temperature until reaches 100% at 700°C over the two catalysts.

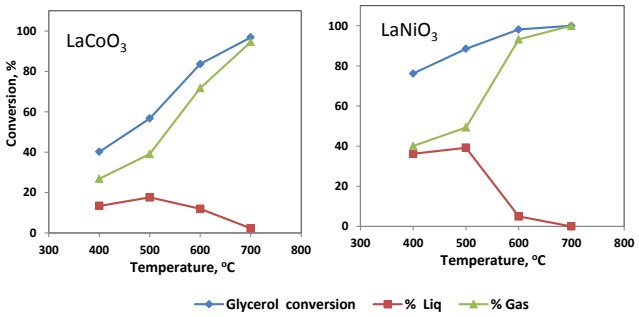

Figure. 5: Temperature profile of catalytic activity of perovskite catalysts.

In GSR process different proposed reaction occurred producing different possible species. ***Gaseous species*** as glycerol ($C_3H_8O_3$), water (H_2O), hydrogen (H_2), carbon monoxide (CO), carbon dioxide (CO_2), methane (CH_4), ethylene (C_2H_4), and ethane (C_2H_6). ***Liquid species*** as acetaldehyde (CH_3CHO), 2-oxopropanal ($C_3H_4O_2$), acrylaldehyde (C_3H_4O), hydroxyacetone ($C_3H_6O_2$), and glyceraldehydes ($C_3H_6O_3$). Also, carbon (graphite, C) can be produced as the ***solid substance*** [28]. The glycerol conversion to gaseous products (X_{gas}) increases by increasing the temperature (Fig. 5), considering the endothermic nature of the overall steam reforming reaction [29]. In contrast, the conversion of glycerol to liquid products through the different reaction routes (as glycerol hydrogenolysis) was expected to be increase at low reaction temperatures due to the exothermic character of such reactions [30, 31]. The proposed reactions occur during GSR reaction can summarized as:

Overall glycerol steam reforming reaction:

$$C_3H_8O_3 + 3H_2O \rightarrow 7H_2 + 3CO_2 \qquad \Delta H^0 = +128 kJ/mol \qquad (1)$$

Thermal decomposition reaction:

$$C_3H_8O_3 \longrightarrow 3CO + 4H_2 \qquad \Delta H^0 = +250 kJ/mol \qquad (2)$$

$$C_3H_8O_3 \rightarrow C_2H_4 + CO + 2H_2O \qquad \Delta H^0 = +41.0 \text{ kJ/mol} \qquad (3)$$

Water-gas shift (WGS) reaction:

$$CO + H_2O \rightarrow CO_2 + H_2 \qquad \Delta H^0 = -41 kJ/mol \qquad (4)$$

Methanation reaction:

$$CO + 3H_2 \rightarrow CH_4 + H_2O \qquad \Delta H^0 = -206 kJ/mol \qquad (5)$$

$$CO_2 + 4H_2 \rightarrow CH_4 + 2H_2O \qquad \Delta H^0 = -164.7 \text{ kJ/mol} \qquad (6)$$

CO_2 reforming of Methane:

$$CH_4 + CO_2 \rightarrow CO + 2H_2 \qquad \Delta H^0 = +247 \text{ kJ/mol} \qquad (7)$$

Oxidative coupling of Methane:

$$2CH_4 + CO_2 \rightarrow C_2H_6 + CO + H_2O \qquad \Delta H^0 = +106 \text{ kJ/mol} \qquad (8)$$

Oxidative coupling of Methane:

$$2CH_4 + 2CO_2 \rightarrow C_2H_4 + 2CO + 2H_2O \qquad \Delta H^0 = +284 \text{ kJ/mol} \qquad (9)$$

Dehydrogenation of ethane:

$$C_2H_6 \rightarrow C_2H_4 + H_2 \qquad \Delta H^0 = +136.33 \text{ kJ/mol} \qquad (10)$$

Hydrogenation of ethylene:

$$C_2H_4 + H_2 \rightarrow C_2H_6 \qquad \Delta H^0 = -137.1 \text{ kJ/mol} \qquad (11)$$

Decomposition of ethylene:

$$C_2H_4 \rightarrow 2C + 2H_2 \qquad \Delta H^0 = -52.4 \text{ kJ/mol} \qquad (12)$$

Disproportion reaction:

$2CO \rightarrow C + CO_2$ $\Delta H^0 = -172.4$ kJ/mol (13)

Methane decomposition:

$CH_4 \rightarrow C + 2H_2$ $\Delta H^0 = +74.6$ kJ/mol (14)

Hydrogenation of CO:

$CO + H_2 \rightarrow C + H_2O$ $\Delta H^0 = -131.3$ kJ/mol (15)

Hydrogenation of CO_2:

$CO_2 + 2H_2 \rightarrow C + 2H_2O$ $\Delta H^0 = -90.1$ kJ/mol (16)

Actually, the equilibrium constant of reaction determines the extent to which the reaction occurs. So, the equilibrium constants of those possible reactions over $LaNiO_3$ and $LaCoO_3$ are calculated and represented as a function of temperature in Fig. (6). The figure shows that, the dehydration of glycerol, to produce C_2H_4, CO and H_2O, is limited within the whole investigated temperature, especially over $LaCoO_3$ catalyst owing to high -Ln K and +ΔG values, as shown in Fig. (6). While, glycerol steam reforming is favorable and strongly spontaneous reaction at any reaction temperature over both $LaNiO_3$ and $LaCoO_3$ catalysts, when, Ln K is large enough and ΔG is negative at all reaction temperatures (Fig. 6). The decomposition of glycerol to form CO and H_2 are also favorable over two catalysts and strongly spontaneous over a $LaCoO_3$ catalyst than over $LaNiO_3$ one, as indicated by the high -□ G value in case of $LaCoO_3$.

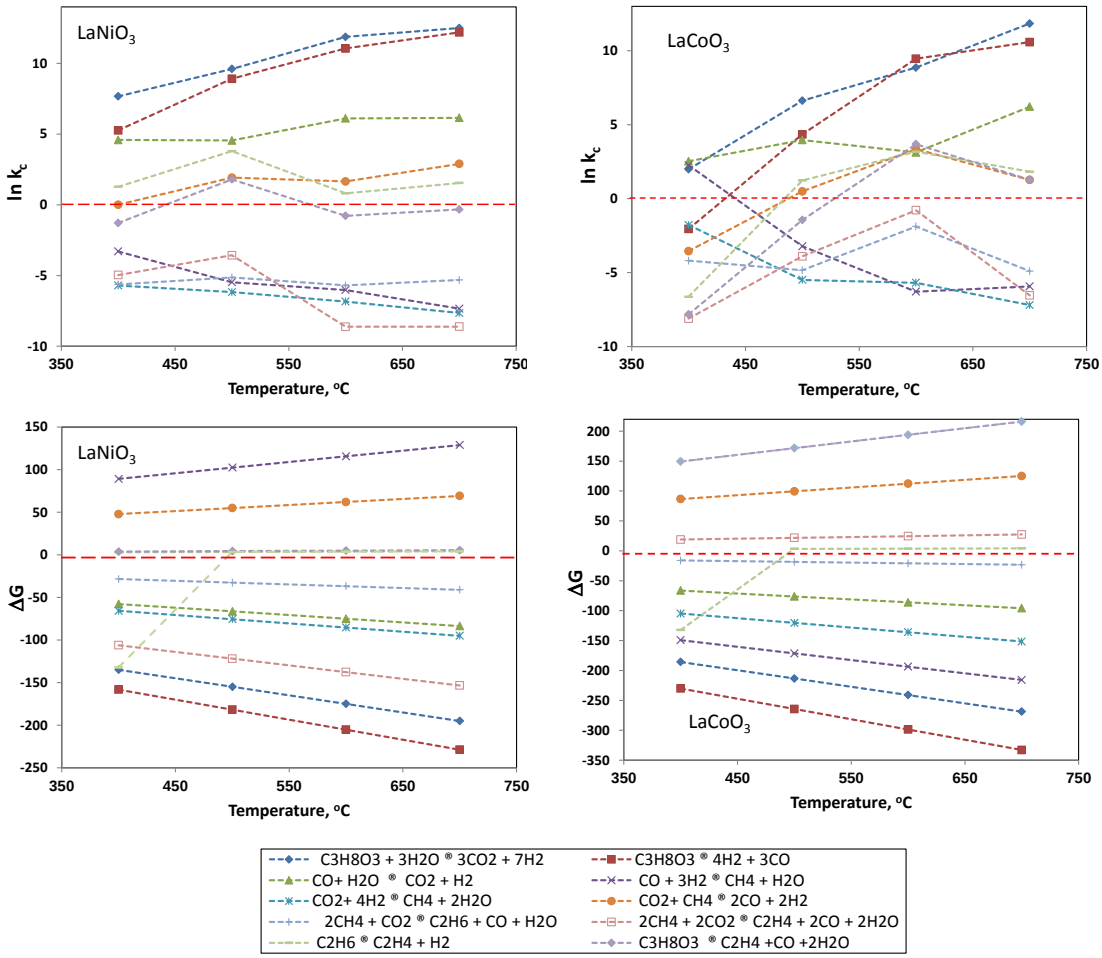

Figure. 6: Ln K and ΔG values for all of the proposed reactions during GSR over $LaNiO_3$ and $LaCoO_3$ catalysts

In contrast, by study the effect of temperature on H_2 yield and H_2 selectivity (Figs. 7), the H_2 yield increased (from 0.11 to 3.15 for $LaNiO_3$ and 0.01 to 1.33 for $LaCoO_3$) as the reaction temperature increase from 400 to 700°C, due to

the endothermic nature of this reaction as indicated by the positive □ H value (Table 2). The highest H₂ selectivity at 700°C achieved 68% for $LaNiO_3$ and 48% for $LaCoO_3$. This phenomenon can be attributed to the large CO produced during the decomposition of glycerol over $LaCoO_3$, increasing the ability to methanation reaction (reaction 5), as confirmed by -□ G value of this reaction over $LaCoO_3$ catalysts. The water gas shift reaction (reaction 4) is limited over the two catalysts owing to law LnK value, and its rate increase with increase in reaction temperature due to the endothermic nature (Table 7).

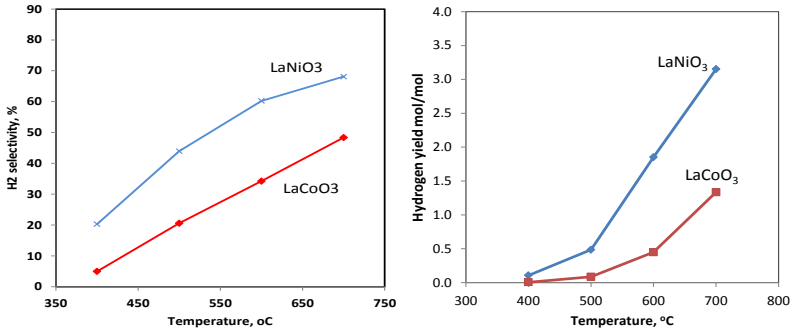

Figure . 7: Temperature profile of H_2 selectivity and H_2 Yield

Fig. 8 shows, methane yield over the two catalysts as a function of temperature. CH_4 production decreases when the temperature increase due to their exothermic nature (-ΔH value) as shown in Table (2). The methane yield was higher over $LaCoO_3$ than over $LaNiO_3$ catalyst. This related to the high Ln K and -ΔG values of the methanation reaction (reaction 5) over $LaCoO_3$, while, lower Ln K and +ΔG values of this reaction over $LaNiO_3$. And, also related to the consumption of methane during the spontaneous CO_2 reforming of methane (reaction 7) over $LaNiO_3$ (high -ΔG value) as shown in Fig. (6). Moreover, the decrease in CH_4 yield with increase in CO, CO_2, and H_2 as the temperature increase, can be attributing to methane steam reforming reaction.

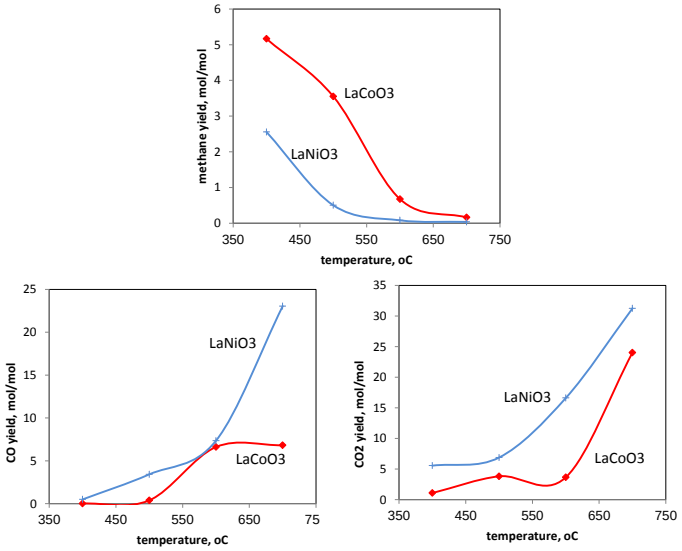

Figure. 8: Methane and CO_2 yields over the two catalysts

CO_2 Oxidative coupling of methane (reactions 8, 9) and ethane dehydrogenation reactions (reactions 10) are other important reactions can occur during GSR reaction. However, the equilibrium limitations (very low LnK value) of those reactions over $LaNiO_3$ and $LaCoO_3$ catalysts confirm the very low yield of ethane and ethylene that formed only at very high temperatures, due to the endothermic nature of both reactions (Table 2).

Table.2 : Thermodynamic parameter for all possible reaction during GSR process over the prepared preovskite catalysts

	$LaNiO_3$, mol		$LaCoO_3$, mol	
	ΔH, j mol^{-1}	**ΔS, j mol^{-1} K^{-1}**	**ΔH, j mol^{-1}**	**ΔS, j mol^{-1} K^{-1}**
$C_3H_8O_3 + 3H_2O \rightarrow 3CO_2 + 7H_2$	91.992	200.504	173.989	276.357
$C_3H_8O_3 \rightarrow C_2H_4 + CO + 2H_2O$	5.483	-5.597	186.336	-221.756
$C_3H_8O_3 \rightarrow 4H_2 + 3CO$	127.145	235.242	238.977	342.308
$CO + H_2O \rightarrow CO_2 + H_2$	33.483	85.955	53.313	98.685
$CO + 3H_2 \rightarrow CH_4 + H_2O$	-69.789	-132.425	-156.870	221.648
$CO_2 + 4H_2 \rightarrow CH_4 + 2H_2O$	-34.637	97.687	-91.884	155.697
$CO_2 + CH_4 \rightarrow 2CO + 2H_2$	46.430	-70.968	101.179	-128.501
$2CH_4 + CO_2 \rightarrow C_2H_6 + CO + H_2O$	2.441	42.239	7.200	23.984
$2CH_4 + 2CO_2 \rightarrow C_2H_4 + 2CO + 2H_2O$	-83.960	157.518	55.085	-27.982
$C_2H_6 \rightarrow C_2H_4 + H_2$	-9.040	-4.260	159.638	196.796

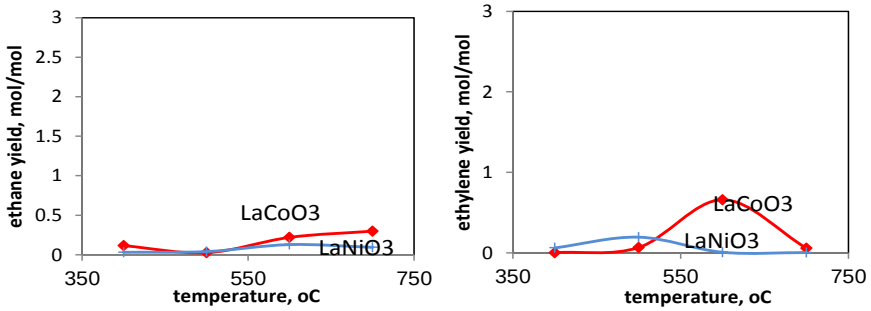

Figure. 9: Ethane and Ethylene yields over the two catalysts

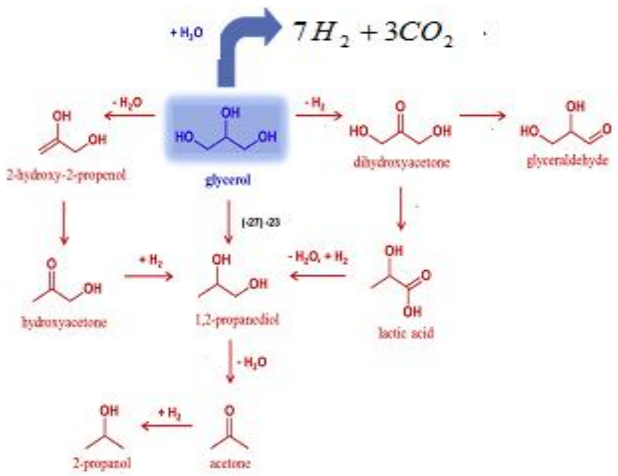

Scheme 1: Dumesic and Simonetti scheme

The product distribution can be explained based on Dumesic and Simonetti mechanism (Scheme 1). They concluded that, the conversion of glycerol to hydrogen takes place through the formation of intermediate species either alcohols or ketones according to the following pathways: dehydrogenation reactions to dihydrixoxyacetone, which

consequently convert to glyceraldehyde and/or lactic acid, the lactic acid reduction form propanediol, and dehydration reactions to 2-hydroxy-2-propenol then to hydroxyacetone forming propanediol. The two path reactions are exothermic reaction (low –ΔG value), so, all mentioned species may be present during the catalytic processing at the lower reaction temperatures [32].

3.3. Catalysts stability and carbon deposition

It was found that at reaction temperature ≥ 600°C, the H_2/CO_2 value equal 2.3 (mol/mol) (Fig. 10) is quite close to the theoretical one (Reaction 1), which indicate that the reaction is mainly steam reforming. Thus, this temperature was chosen to perform the time on stream (TOS) for the two catalysts.

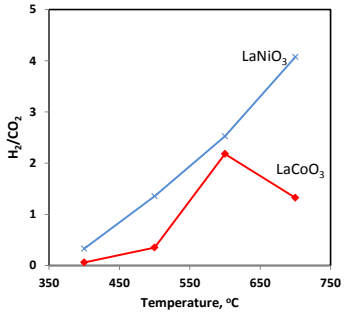

Figure. 10: Temperature profile Vs. H_2/CO_2

TOS screened out during 16 h at 650°C for $LaNiO_3$ and $LaCoO_3$ (Fig. 11). The selectivity of H_2 production increases at the initial 6 h on using the two catalysts, and then goes dramatically decrease for $LaNiO_3$ while keeping stable in case of $LaCoO_3$ in the rest 10 h. On the other hand, higher CO_2 selectivity generally corresponds to lower CO selectivity, which is usually deemed as the criterion for determining the activity of water-gas shift reaction (WGSR). Hence, the variation tendency of WGSR activity of catalysts agrees well with that of the H_2 yield, and this in turn proves that WGSR has an important influence on the product distributions [14]. This explains the variations in the stability of the two catalysts, i.e the $LaCoO_3$ is a most active catalyst for WGSR than $LaNiO_3$.

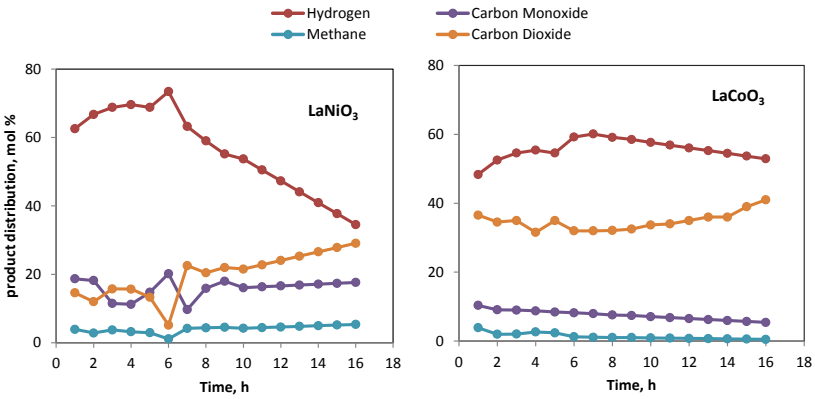

Figure. 11: Temperature profile of time on stream for perovskite catalysts

The diffraction patterns of the spent catalysts (Fig. 12), representes strong characteristic peaks of $La_2O_2CO_3$ according to JCPDS (48-1113) [33]. This may be attributed to the fact that part of the CO_2 generated during the reaction is absorbed by La_2O_3, forming a carbonate, i.e. carbon species formed on Ni and Co sites may then have been removed by oxygen species originating from the carbonate, such as $La_2O_2CO_3$ [34]. TEM images of spent catalysts $LaNiO_3$ (Fig.13) show a carbon nanotube (CNT) while for $LaCoO_3$ has a coke deposition. The amount of carbon deposits was found to be 0.83 and 0.03 for $LaNiO_3$ and $LaCoO_3$ respectively as verified by TGA/DTA (Fig.13) an exothermic peak

appeared at high temperature (500°C) in case of $LaNiO_3$ is due to the formation of carbon nanotube CNTs, which is in agreement with the TEM data. On the other hand deposits of carbon can be formed via the dissociation of CH_4 ($CH_4 \Leftrightarrow C + 2H_2$). Therefore, the relatively low carbon deposits in parallel with the low yield of CH_4 during the glycerol steam reforming process.

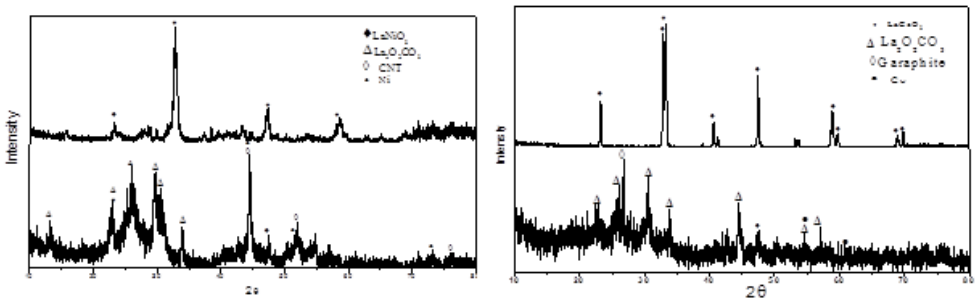

Figure. 12: X-Ray diffraction pattern for spent $LaNiO_3$ & $LaCoO_3$ samples

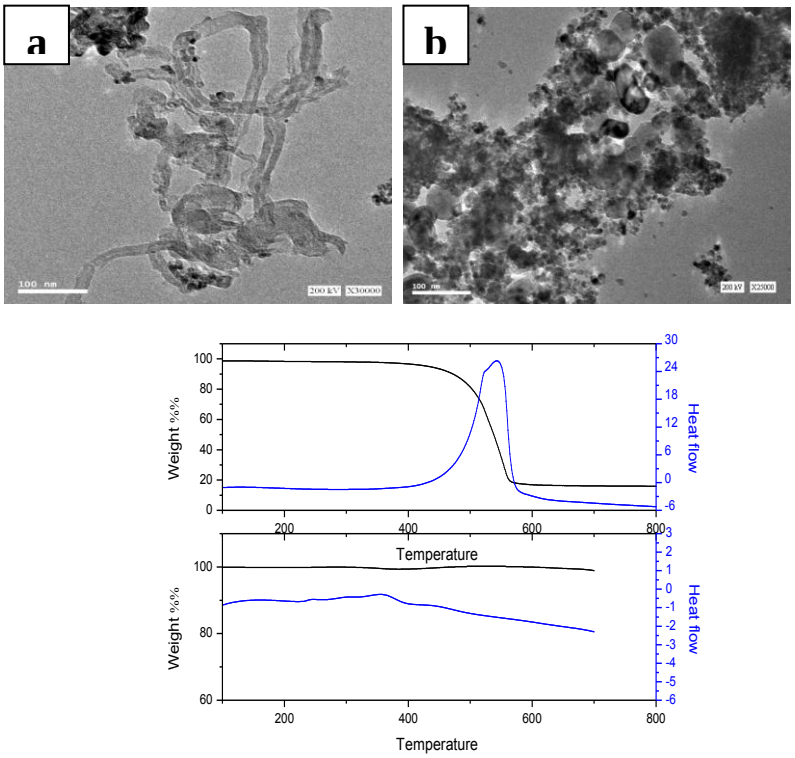

Figure. 13: TEM image and DTA/TGA for spent (a) $LaNiO_3$ and (b) $LaCoO_3$ samples

The carbon deposition at the catalyst's surface was taking place during different reactions:

$2CO_{(g)} \leftrightarrow CO_{2(g)} + C_{(s)}$ (17)

$CH_{4(g)} \leftrightarrow 2H_{2(g)} + C_{(s)}$ (18)

$CO_{(g)} + 2H_{2(g)} \leftrightarrow H2O_{(g)} + C_{(s)}$ (19)

$CO_{2(g)} + 2H_{2(g)} \leftrightarrow 2H_2O_{(g)} + C_{(s)}$ (20)

Cheng et. al. [35], suggested that, at lower reaction temperature, carbon produces due to hydrogenation reaction (of CO2 or CO) and/or disproportionation reaction. While at higher temperature, carbon is more likely to be produced from methane decomposition reaction.

3.5. Calorific value of GSR reaction

From the composition of gas samples, the calorific value was estimated, bearing in mind the specific gravity (Sp Gr), high heat value, and low heat value of each of the gas species according to the American standard test method (ASTM-3588). The gases generated in the glycerol steam reforming process have a calorific value expressed by Btu/ft^3 for mole% and Kj/Kg for weight%. Data in Table (3) established moderate calorific value due to the CO_2 value (15-80 mol %) which increases with rising the reaction temperature. On using $LaNiO_3$ catalyst, the calorific value of the products increases with the increase in reaction temperatures until reaching a high value of 284.706 Btu/ft^3 at 700^{o}C due to the high yield of H_2 and low CO_2 yield. While on using $LaCoO_3$ the calorific value reached a higher value of 434.785 Btu/ft^3 at 600^{o}C due to the low CO_2 yield (15 mol %) [36].

Table. 3: Calorific Value data of the gas samples

	$LaNiO_3$				**$LaCoO_3$**			
	400	**500**	**600**	**700**	**400**	**500**	**600**	**700**
Gross CV, Btu/ft^3	222	257	280	285	204	180	435	239
Gross CV, Kj/Kg	5,880	10,832	16,147	20,197	4,615	4,929	18,308	10,288
Net CV, Btu/ft^3	164	226	245	248	186	147	360	209
Net CV, Kj/Kg	5,306	9,669	4,121	17,608	4,196	4,433	16,817	9,046

4. Conclusion

The analysis of thermodynamic parameter for glycerol steam reforming reaction over two peroveskite nanocatalysts ($LaNiO_3$ and $LaCoO_3$) has been performed to study the effect of reaction temperature on product distribution at atmospheric pressure for production of pure hydrogen. The equilibrium constant and thermodynamic parameter calculation indicate that, the dehydration of glycerol, to produce C_2H_4, CO and H_2O, is limited within the whole investigated temperature owing to high -Ln K and +ΔG values. While, glycerol steam reforming is favorable at any reaction temperature over both $LaNiO_3$ and $LaCoO_3$ catalysts, When, Ln K is large enough and ΔG is negative. Hydrogen production, enhanced over $LaNiO_3$ than $LaCoO_3$ at the same reaction temperature. In addition, $LaCoO_3$ provided more deactivation resistant along to 16h than $LaNiO_3$. XRD results for the spent catalyst emphasized that the main phase formed in the two catalysts is $La_2O_2CO_3$, due to the existence of the CO_2 in the reaction product, in agreement with TEM and TGA/DTA results. Moreover, On using $LaNiO_3$, the produced product at 700^{o}C was found to have a moderate calorific value (284.706 Btu/ft^3) as compared to high calorific value on using $LaCoO_3$ (434.785 Btu/ft^3) at 600^{o}C due to the low yield of CO_2 (15 mol %). Nevertheless, the work can consider as an important step for further development of the technology of hydrogen production from glycerol feedstock, as biodiesel byproduct, using cheap and stable proveskite nano-catalysts.

References

[1] M. Di Braccio, G. Grossi, G. Roma, L. Vargiu, M. Mura, M. Elena Marongiu, *Eur. J. Med. Chem*., 36 (2001) 935-949.

[2] K. Kiec-Kononowicz, J. Karolak-Wojciechowska, C. E. Müller, B. Schumacher, E. Pekala, E.Szymanska, *Eur. J. Med. Chem*., 36 (2001) 407-419.

[3] V. Crupi, D. Majolino, M. R. Mondello, P. Migliardo, V. Venuti, *J. Pharm. Biomed. Anal.*, 29 (2002) 1149-1152.

References

[1] L.F. Bobadilla, A. Alvarez, M.I. Dominguez, F. Romero-Sarria, M.A. Centeno, M. Montes, J.A. Odriozola: *Appl. Catal. B* 123–124 (2012) 379.

[2] F. Ma, M.A. Hanna: *Bioresour Technol.*, 70 (1999) 1–15.

[3] N. Rahmat, A.Z. Abdullah, A.R. Mohamed: Renew. Sustain. *Energ. Rev.* 14 (2010) 987.

[4] C. Wang, B.L. Dou, H.S. Chen, Y.C. Song, Y.J. Xu, X. Du: *Int. J. Hydr. Energ.*, 38 (2013) 3562.

[5] C. Wang, B.L. Dou, H.S. Chen, Y.C. Song, Y.J. Xu, X. Du: *Chem. Eng. J.* 220 (2013) 133.

[6] C.D. Dave, K.K. Pant: *Renew. Energ.* 36 (2011) 3195.

[7] A. Iriondo, V.L. Barrio, M. El-Doukkali, J.F. Cambra, M.B. Güemez, J. Requies: *Int. J. Hydr. Energ.* 37 (2012) 2028.

[8] L. He, J.M.S. Parra, E.A. Blekkan, D. Chen: *Energ. Environ. Sci.* 3 (2010) 1046.

[9] B. Dou, C. Wang, H. Chen, Y. Song, B.Xie: *Int. J. Hydrogen Energy* 38 (2013) 11902.

[10] L.V. Mattos, G. Jacobs, B.H. Davis, F.B. Noronha: *Review of Reaction Mechanism and Catalyst Deactivation Chemical Reviews* 112 (2012) 4094.

[11] D. R. Abd El-Hafiz, M. A. Ebiad, Radwa A. El-salamony: *Mater Renew Sustain Energy* 3 (2014)34.

[12] M. A. Ebiad, D. R. Abd El-Hafiz, R. A. Elsalamony, L. S. Mohamed: *RSC Advances*, 2 (2012) 8145.

[13] R. A. Elsalamony, D. R. Abd El-Hafiz, M. A. Ebiad, A. M. Mansour, L. S. Mohamed: *RSC Adv.*, 3 (2013) 23791.

[14] G. Wu, S. Li, C. Zhang, T. Wang, J. Gong: *Appl. Catal. B* 144 (2014) 277–285.

[15] L. Wei, K. Liy, Y.C. Maz: *Intern. J. Chem. React. Eng.*, 10 (2012) 79.

[16] N. Aishah, S. Amin, et. al.: *Jurnal Teknologi (Sciences & Engineering)* 67:3 (2014) 109.

[17] M.R. Nanda, Z.S. Yuan, W.S. Qin, H.S. Ghaziaskar, M.A. Poirier, C.C. Xu: *Fuel* 117 (2014) 470.

[18] D. Karthikeyan, G.S. Shin, D.J. Moon, J.H. Kim, N.C. Park, Y.C. Kim: *J. Nanosci. Nanotechnol.* 11 (2011) 1443.

[19] G.D. Wen, Y.P. Xu, H.J. Ma, Z.S. Xu, Z.J. Tian: *Int. J. Hydrogen Energy* 33 (2008) 6657.

[20] S. Tatenoa, K. Hirosea, N. Sata, Y. Ohishi: *Physics of the Earth and Planetary Interiors* 181 (2010) 54.

[21] (a) D. Aman, T. Zaki, S. Mikhail, S.A. Selim: *Catal. Tod.*, 164 (2011) 209.

(b) D. Aman, T. Zaki, S. Mikhail, M. Ali,: *Chem. Proc. Eng. Res.* 23 (2014) 29.

[22] S. M. De Lim, A.M. Silv, L.Cost, M. Jose, J.M. Assaf, R.S. Mattos, A. Venugopal, F.B. Noronha: *Appl. Catal. B.* 121-122, (2012)1.

[23] N. Mota, M.C. Alvarez-Galvan, R.M. Navarro, S.M. Al-Zahrani, A. Goguet, H. Daly, W. Zhang, A. Trunschke, R. Schlögl, J.L.G. Fierro: *Appl. Catal. B.* 113–114 (2012) 271.

[24] S. Brunauer, L.S. Deming, W.S. Deming, E. Teller: *J.Amer. Chem. Soc.* 62 (1940) 1723.

[25] S.J. Greeg, K.S.W. Sing, IUPAC manual of symbols and terminology, a manual entitled "Reporting physisorption data for gas/solid systems with special reference to the determination of surface area and porosity", appendix 2 part I, Prowisional, *Coll. Sur. Chem.* 31, 578, (1972).

[26] S. Adhikari, S. Fernando, S.R. Gwaltney T.S. Filip, R.B. Mark, P. Steele: *Int. J. Hydrogen Energy*, 32 (2007) 2875.

[27] S. Adhikari, S. Fernando, A.A. Haryanto: *Energy Fuels*, 21 (2007) 2306.

[28] F. Pompeo, G. Santori, N.N. Nichio: *Int J. Hydrogen Energy*, 35 (2010) 8912.

[29] Y. Cui, V. Galvita, L. Rihko-Struckmann, H. Lorenz, K. Sundmacher, *Appl. Catal. B* 90 (2009) 29–37.

[30] C.K. Cheng, S.Y. Foo, A.A. Adesina: *Catal. Commun.* 12 (2010) 292.

[31] C.A. Franchini, W. Aranzaez, A. M. Duarte de Farias, G. Pecchi, M. A. Fraga: *Appl. Catal. B.*, 147 (2014) 193.

[32] D.A. Simonetti, J.A. Dumesic: *Cat. Rev. Sci. Eng.*, 51 (2009), 441.
[33] C. Wang, Y. Yang, Z. Zhang, F. Liao, J. Ju, Z. Shi, J. Lin, Y. Li, F. Huang: *Mater. Lett. 134* (2014) 176.
[34] V.V. Thyssen, T.A. Maia, E.M. Assaf: *Fuel* 105 (2013) 358.
[35] C.K. Cheng, S.Y. Foo, A.A. Adesina: *Intern. J. hydrog. energy* 37 (2012) 10101.
[36] C. Diez, O. Martinez, L.F. Calvo, J. Cara, A. Moran: *Waste Management* 24 (2004) 463.